JACS
JOURNAL OF THE AMERICAN CHEMICAL SOCIETY

Communication

pubs.acs.org/JACS

Tunable Catalysts for Solvent-Free Biphasic Systems: Pickering Interfacial Catalysts over Amphiphilic Silica Nanoparticles

Wen-Juan Zhou,*[,†,‡] Lin Fang,[†] Zhaoyu Fan,[†] Belén Albela,[‡] Laurent Bonneviot,[‡] Floryan De Campo,[†] Marc Pera-Titus,*[,†] and Jean-Marc Clacens[†]

[†]Eco-Efficient Products and Processes Laboratory (E2P2L), UMI 3464 CNRS−Solvay, 3966 Jin Du Road, Xin Zhuang Ind. Zone, 201108 Shanghai, China

[‡]Laboratoire de Chimie, UMR 5182 CNRS−Ecole Normale Supérieure de Lyon, 46 allée d'Italie, 69364 Lyon, France

Supporting Information

ABSTRACT: Stabilization of oil/oil Pickering emulsions using robust and recyclable catalytic amphiphilic silica nanoparticles bearing alkyl and propylsulfonic acid groups allows fast and efficient solvent-free acetalization of immiscible long-chain fatty aldehydes with ethylene glycol.

Clean and efficient conversion of biobased raw materials into fine chemicals and transportation fuels is a key challenge in the design of biorefineries.[1] Typical organic syntheses using fatty derivatives and polyols usually encompass the reaction of immiscible reagents.[2] To circumvent this issue, a combination of a surfactant and a homogeneous catalyst or even a hybrid surfactant-combined-catalyst (i.e., dodecyl benzene sulfonic acid[3] or amphiphilic organocatalysts[4]) can favor the contact and transfer between reagents though in detriment of recycling.

Amphiphilic nanoparticles can stabilize emulsions (i.e., Pickering emulsions), allowing facile separation and recycling after operation.[5] Appropriate functionalization of their surface may combine both surfactant and catalytic properties at the interface of both phases called here Pickering Interfacial Catalysis (PIC). In a pioneering study, Resasco et al. promoted Pickering emulsions with amphiphilic particles combining hydrophobic single-walled carbon nanotubes (SWCNTs) and hydrophilic silica, also incorporating catalytic sites (i.e., Pd nanoparticles and alkali moieties).[6] The emulsions could selectively catalyze the simultaneous aldol condensation−hydrogenation reaction of 5-methylfurfural and acetone in water/oil biphasic systems with controlled phase selectivity. The authors further extended the concept to hydrogenation and partial oxidation reactions using interfacial catalysts based on multiwalled CNTs grown on alumina, 'onion-like' carbon (OC) on silica, and Janus solids supporting metal nanoparticles (Pd and Cu)[7] as well as to acid-catalyzed alcohol dehydration reactions and *m*-cresol alkylation with 2-propanol using hydrophobic HY zeolites.[8]

Other examples of the PIC concept comprising hybrid carbon materials for biofuel upgrading include Au@PHCS (PHCS = porous hollow carbonaceous spheres), Ru@pristine-CNT, Pd@CN (CN = N-doped mespoporous carbon), iron oxide/CNT, CNT/TiO_2, and Ag/graphene oxide.[9] Very recent noncarbon amphiphilic nanoparticles with proven PIC properties include alkylammonium cations combined with a polyoxometalate $[PW_{12}O_{40}]_3$ anion,[10] layered niobate $K_4Nb_6O_{17}$ intercalated with alkylammonium cations,[11] Fe_2O_3/FeOOH red mud derivates,[12] and polymersomes and nanocages hosting enzymes.[13]

Despite the above developments, few reports are available on biphasic oil/oil systems, though commonly found upon biomass upgrading.[14] Herein we intend to fill this gap using the solvent-free acid-catalyzed acetalization reaction of immiscible long-chain fatty aldehydes ($n > 9$) with ethlylene glycol (EG) as an illustrative example, for which little literature is available.[15] To this aim, we rationally designed amphiphilic silica nanoparticles functionalized with propylsulfonic and alkyl groups with variable chain lengths (Figure 1A). The sulfonic acid groups served not only as active sites but also as hydrophilic moieties for tuning the amphiphilic properties of the particles.

The amphiphilic silica nanoparticles were prepared by a coprecipitation method (see SI for experimental details). The synthesis protocol included three main steps: (1) co-condensation of tetraethyl orthosilicate (TEOS) with organosilanes and (3-mercaptopropyl)trimethoxysilane with a molar ratio of 16:4:1 and a variable carbon length C*n* (n = 3, 8, 18, i.e., trimethoxy(propyl)silane, trimethoxy(octyl)silane, trimethoxy(octadecyl)silane) under alkaline conditions using ethanol and water as cosolvents; (2) oxidation of thiol (−SH) groups into sulfonate ($-SO_3X$, X = NH_4^+, Na^+) using aqueous hydrogen peroxide; and (3) acidification to obtain sulfonic acid-functionalized particles. Three samples with different alkyl chain lengths were prepared (i.e., C_3, C_8, and C_{18}), hereinafter referred to as SiNP_SO3H_C3, SiNP_SO3H_C8, and SiNP_SO3H_C18, respectively. The mean particle size was in each case 166, 153, and 310 nm (±5 nm) (Figure S1) for effective C*n*/sulfonic molar ratios of 0.1, 5.5, and 7.9, respectively. The density of alkyl moieties was 0.2, 11.0, and 20.3 groups/nm^2 for SiNP_SO3H_C3, SiNP_SO3H_C8, and SiNP_SO3H_C18, respectively, whereas the density of SiOH groups was in each case 12.7−14.6, 14.3−23.2, and 33.5−51.2 groups/nm^2 according to complementary information from TGA and quantitative ^{29}Si solid-state NMR (Table S1). Such high densities of alkyl and SiOH groups indicate the formation of organic layers partially incorporating with the inorganic silica

Received: January 29, 2014
Published: March 18, 2014

   dx.doi.org/10.1021/ja501019n | *J. Am. Chem. Soc.* 2014, 136, 4869−4872

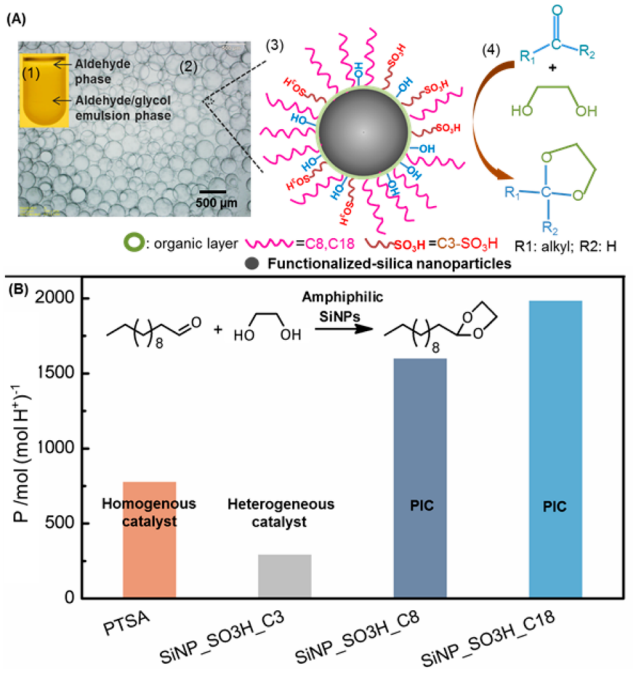

Figure 1. (A) Biphasic acetalization reaction catalyzed by amphiphilic silica nanoparticles under PIC. (A1) Picture of the solution using 50 v/v % EG and 50 v/v % aldehyde and 1.7 wt % SiNP_SO3H_C18 after homogenization at 60 °C for 15 min; (A2) typical optical micrographs of the emulsions; (A3) scheme of amphiphilic silica nanoparticles located at the aldehyde/EG interface; (A4) scheme of the catalytic action of sulfonic acid sites nearby hydrophobic chain on acetalization of aldehyde by EG. (B) Productivity for acetalization of C_{12}-aldehyde by EG over PTSA, SiNP_SO3H_C3, SiNP_SO3H_C8, and SiNP_SO3H_C18. Reaction conditions: 60 °C, C_{12}-aldehyde (0.1 mol), EG (0.2 mol), catalyst amount adjusted to provide the same H^+ equivalents (9.5 μmol, particle loading ~1.7 wt % for the solid samples).

core during the synthesis due to the large solubility difference between the organosilanes and TEOS. This phenomenon is not observed in organosilane grafted Aerosil 200 materials, encompassing a lower density of alkyl and SiOH groups.[15]

The acid–base titration of Brønsted acidity provided 0.23, 0.24, and 0.19 mmol$[H^+]$/g for SiNP_SO3H_C3, SiNP_SO3H_C8, and SiNP_SO3H_C18, respectively, matching approximately the sulfur content measured by ICP analysis and indicating that thiol groups were mostly oxidized into sulfonic units (Table S1). A tiny amount of $-S-SO_2-$ species was detected in SiNP_SO3H_C18 as inferred from ^{13}C–CP-MAS NMR (Figure S2). From inverse gas chromatography (IGC), the adsorption/desorption of methylene chloride (CH_2Cl_2) taken as weak basic probe provided specific interaction energies (ISP) of 24.7, 16.5, and 14.6 kJ/mol for SiNP_SO3H_C3, SiNP_SO3H_C8, and SiNP_SO3H_C18, respectively (Table S2 and Figure S3). The trend reflects a decreasing acid strength combining both longer alkyl chains and higher density of SiOH groups. The nondispersive component of the surface energy (γ_s^d, kJ/mol) measured also from IGC showed a trend consistent with lower polarity for longer chains: SiNP_SO3H_C3 (44.4) < SiNP_SO3H_C8 (29.7) < SiNP_SO3H_C18 (28.1) (Table S2). More insights can be further obtained from the adsorption energy distribution functions (AEDF) plotted here for water and methyl chloride (CH_2Cl_2) (Figure S4). Notwithstanding that the distributions for water were similar for the different functionalized silicas, the peak values were displaced to unusually higher energies, providing a direct signature of sulfonic acid groups. The AEDF for methyl chloride showed multiple peaks for SiNP_SO3H_C3 and SiNP_SO3H_C8, suggesting the presence of heterogeneous Si–O–Si sites on both the silica core and the organic layers.

The catalytic activity of the SiNPs was tested in the biphasic acetalization reaction of fatty C_{12}-aldehyde with EG at 60 °C for 1 h under low excess of EG. Benchmark catalysts were also tested, including heterogeneous HZSM-5 and H-Resin. A remarkably higher catalyst productivity (P) to the acetal was achieved on SiNP_SO3H_C8 and SiNP_SO3H_C18, reaching values about 1602 and 1850, respectively, compared to the values of 315 and 348 found for HZSM-5 and H-Resin, respectively (Figure S5). The latter catalysts dispersed preferentially in the EG phase without stirring due to their pronounced hydrophilic behavior, the contact between the two reactants occurring far away from the acid sites. A similar behavior was observed for SiNP_SO3H_C3. In contrast, SiNP_SO3H_C8 localized at the C_{12}-aldehyde/EG interface, whereas SiNP_SO3H_C18 localized both at the interface and in the C_{12}-aldehyde phase (Figure S6), which is consistent with a much better hydrophilic/hydrophobic balance in the latter SiNPs.

The activity of SiNPs was also assessed in comparison to *p*-toluenesulfonic acid (PTSA), a commonly used homogeneous acid catalyst for biphasic reactions. PTSA was indeed more active (P = 750) than SiNP_SO3H_C3 (295), but less than SiNP_SO3H_Cn (n = 8 or 18, P > 1500) (Figure 1B). A comparative kinetic study was conducted for SiNP_SO3H_C18 and PTSA under mild stirring (500 rpm) (Figure 2). The reaction rate was slower with SiNP_SO3H_C18 during

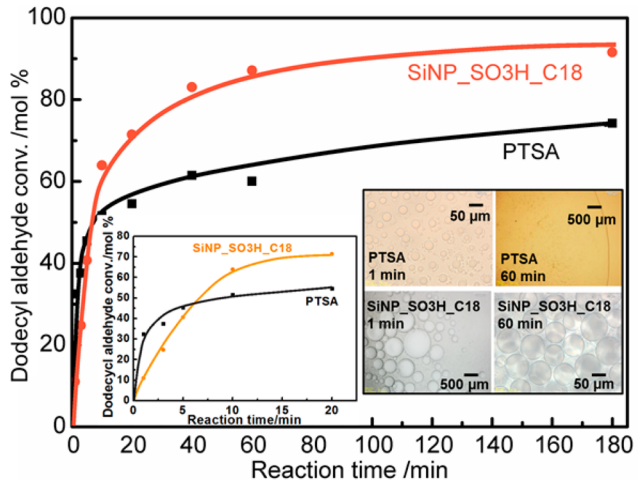

Figure 2. Comparative advancement of the acetalization reaction of C_{12}-aldehyde with EG over SiNP_SO3H_C18 and over PTSA. Left insert: zoom into the 0–20 min period of time. Right insert: Typical optical micrographs of solutions at 1 and 60 min. Reaction conditions as in Figure 1.

the first 5 min while at longer times became faster, reaching almost chemical equilibrium after 1 h (Figure 2 insert left). In contrast, the reaction reached equilibrium only after 24 h with PTSA. A devoted optical microscopy study revealed that a stable C_{12}-aldehyde/EG emulsion was generated under SiNP_SO3H_C18 (and SiNP_SO3H_C8), while no droplets

dx.doi.org/10.1021/ja501019n | J. Am. Chem. Soc. 2014, 136, 4869–4872

were observed under PTSA after 10 min reaction (Figure 2 insert right and Figure S7). Likewise, SiNP_SO3H_C3 was unable to form stable droplets due to its patent hydrophilic behavior, showing a fast phase separation (Figures S7 and S8). This body of results emphasizes the superior ability of amphiphilic SiNP_SO3H_C18 as interfacial catalyst by stabilizing Pickering emulsions.

Since the stirring rate is known to affect the formation of emulsions, the kinetic study was repeated under fast stirring conditions (17,000 rpm). The C_{12}-aldehyde conversion increased in the presence of both PTSA and SiNP_SO3H_C18 (Figure S9). Again, this was after 5 min that catalysis by SiNP_SO3H_C18 overtook PTSA. According to optical microscopy, emulsion droplets were not yet formed in both catalytic systems after 1 min of reaction even under fast stirring. The higher catalytic activity observed for PTSA at very short times is therefore attributed to its partial solubility in both phases. We carried out some additional catalytic tests in the presence of water (40 mol % of C_{12}-aldehyde). The C_{12}-aldehyde conversion decreased from the initial value of 91.6% to 81.0% for SiNP_SO3H_C18 particles, whereas it evolved from 63.0% to 53.0% for PTSA (Table S3). These results indicate that even if water might exert a poisoning effect on the acid sites, this should be similar for both catalysts. Furthermore, the fact that the C_{12}-aldehyde conversion decreases in a similar manner for both catalysts seems to suggest that such reduction is likely attributed to a dilution effect without affecting the emulsification properties (Figure S9). Finally, the addition of the acetal product into the reaction system for an equivalent of 30% yield resulted in the rapid formation of both large and small C_{12}-aldehyde droplets, being observed only after 1 min of reaction at 60 °C (Figure S10). This experiment illustrates the synergistic effect between the acetal and SiNP_SO3H_C18 in the formation of emulsion droplets, increasing its advantage along the reaction and contributing to the inversion of tendency between PTSA and SiNP_SO3H_C18 over time in Figure 2.

To illustrate when and why PIC is preferable over homogeneous catalysis for biphasic acetalization by EG, a comparative study was performed on the reactivity of aldehydes presenting different affinity for EG with respect to the higher distance between their respective Hansen solubility parameters (i.e., Ra, Table S4 and Figure 3). As expected, PTSA showed the highest activity for benzaldehyde acetalization, the latter being fully miscible with EG (Ra = 129). Comparatively, it appeared that the C_7-aldehyde was not hydrophobic enough to promote PIC using SiNP_SO3H_C18, since the system could hardly form an emulsion, whereas PTSA could completely dissolve in the reactants reaching higher reactivity (Figure S11). In contrast, SiNP_SO3H_C18 reached higher activities than PTSA for C_9- and C_{12}-aldehyde, Pickering emulsions taking place in both cases (Figures 2 and S12).

Finally, the reusability of amphiphilic silica nanoparticles was evaluated on the acetalization of C_{12}-aldehyde and benzaldehyde over SiNP_SO3H_C18. After each cycle, the catalyst was separated from the reaction system by centrifugation, washed using ethanol (30 mL, four times), and dried at room temperature. The catalyst did not show any appreciable deactivation even after 3 and 7 consecutive runs, respectively, for each aldehyde (Figure S13).

In summary, we demonstrated that amphiphilic silica nanoparticles with a suitable balance between hydrophilic and hydrophobic properties can behave as efficient interfacial catalysts for the acetalization of fatty aldehydes with EG by stabilizing Pickering emulsions. The catalysts could be recovered by centrifugation after reaction and reused with no appreciable deactivation. The easily tunable hydrophilic/hydrophobic properties of silica nanoparticles open an avenue for the conception *à la carte* of interfacial catalysts for industrially relevant biphasic reactions avoiding the use of solvents. Prospective developments in progress concern the study of amphiphilic catalysts for acid-catalyzed etherification and acetalization reactions of biomass-derived polyols.

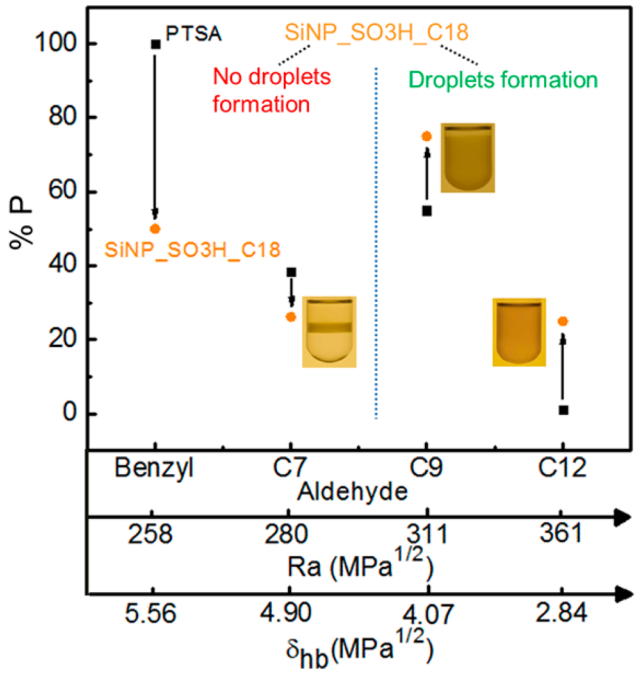

Figure 3. Productivity (P) of acetalization of different aldehydes with EG over SiNP_SO3H_C18 relative to the productivity for the benzaldehyde/EG/PTSA system over PTSA (P = 2038). Bottom: second and third abscissa axes indicating the aldehyde characteristics in terms of distance between Hansen solubility parameters of aldehyde and EG (Ra) and the Hansen solubility component relative to hydrogen bonding (δ_{hb}), respectively (Table S4). Inserts: pictures of the solutions showing the fractions formed in the mixture in the presence of SiNP_SO3H_C18 after emulsification for 20 min at RT. Reaction conditions: 30 °C, 1 h and other reaction conditions as in Figure 1.

■ ASSOCIATED CONTENT

Supporting Information

Textural and surface properties of the modified silicas measured by IGC, collection of aldehyde/EG emulsion images stabilized by amphiphilic silicas, catalytic stability tests, effect of the acetal product and water on the catalytic activity and emulsion formation. This material is available free of charge via the Internet at http://pubs.acs.org.

■ AUTHOR INFORMATION

Corresponding Authors

wenjuan.zhou@solvay.com

marc.pera-titus-ext@solvay.com

Notes

The authors declare no competing financial interest.

dx.doi.org/10.1021/ja501019n | *J. Am. Chem. Soc.* 2014, 136, 4869−4872

■ ACKNOWLEDGMENTS

This work was funded by CNRS and Solvay through the BioSurf project. The authors would like to express their gratitude to Dr. Eric Brendle for helpful discussions on IGC and Dr. Bingwen Hu for solid-state NMR measurements.

■ REFERENCES

(1) (a) Corma, A.; Iborra, S.; Velty, A. *Chem. Rev.* **2007**, *107*, 2411. (b) Bozell, J. J.; Petersen, G. *Green Chem.* **2010**, *12*, 539. (c) Gallezot, P. *Chem. Soc. Rev.* **2012**, *41*, 1538. (d) Alonso, D. M.; Wettstein, S. G.; Dumesic, J. A. *Chem. Soc. Rev.* **2012**, *41*, 8075.

(2) Fischmeister, C.; Bruneau, C.; De Oliveira Vigier, K.; Jérôme, F. Catalytic conversion of biosourced raw materials: homogeneous catalysis. In *Biorefinery: From Biomass to Chemicals and Fuels*; Aresta, M., Dibenedetto, A., Dumeignil, F., Eds.; De Gruyter: Berlin, 2012, p 231.

(3) Gaudin, P.; Jacquot, R.; Marion, P.; Pouilloux, Y.; Jérôme, F. *ChemSusChem.* **2011**, *4*, 719.

(4) (a) Li, C.; Gao, J.; Jiang, Z.; Wang, S.; Lu, H.; Yang, Y.; Jing, F. *Topics Catal.* **2005**, *35*, 169. (b) Zhong, L.; Gao, Q.; Gao, J.; Xiao, J.; Li, C. *J. Catal.* **2007**, *250*, 360. (c) Li, J.; Zhang, Y.; Han, D.; Jia, G.; Gao, J.; Zhong, L.; Li, C. *Green Chem.* **2008**, *10*, 608. (d) Zhang, B.; Jiang, Z.; Zhou, X.; Lu, S.; Li, J.; Liu, Y.; Li, C. *Angew. Chem., Int. Ed.* **2012**, *51*, 13159. (e) Xu, J.; Zhao, S.; Ji, Y.; Song, Y.-F. *Chem.—Eur. J.* **2013**, *19*, 709.

(5) (a) Binks, B. P. *Curr. Opin. Colloid Interface Sci.* **2002**, *7*, 21. (b) Walstra, P. Emulsions, In *Fundamentals of Interface and Colloid Science* 1st ed., Lyklema, J., Ed.; Elsevier: Amsterdam, 2005; Vol *5*, pp 8.2−8.92. (c) Aveyard, R.; Binks, B. P.; Clint, J. H. *Adv. Colloid Interface Sci.* **2003**, *100−102*, 503. (d) Leal-Calderon, F.; Schmitt, V. *Curr. Opin. Colloid Interface Sci.* **2008**, *13*, 217.

(6) Crossley, S.; Faria, J.; Shen, M.; Resasco, D. E. *Science* **2010**, *327*, 68.

(7) (a) Faria, J.; Ruiz, M. P.; Resasco, D. E. *Adv. Synth. Catal.* **2010**, *352*, 2359. (b) Ruiz, M. P.; Faria, J.; Shen, M.; Drexler, S.; Prasomsri, T.; Resasco, D. E. *ChemSusChem.* **2011**, *4*, 964. (c) Drexler, S.; Faria, J.; Ruiz, M. P.; Harwell, J. H.; Resasco, D. E. *Energy Fuels* **2012**, *26*, 2231. (d) Zapata, P. A.; Faria, J.; Ruiz, M. P.; Resasco, D. E. *Top. Catal.* **2012**, *55*, 38. (e) Shi, D.; Faria, J. A.; Rownaghi, A. A.; Huhnke, R. L.; Resasco, D. E. *Energy Fuels* **2013**, *27*, 6618.

(8) Zapata, P. A.; Faria, J.; Ruiz, M. P.; Jentoft, R. E.; Resasco, D. E. *J. Am. Chem. Soc.* **2012**, *134*, 8570.

(9) (a) Yang, X.; Wang, X.; Qiu, J. *Appl. Catal. A: General* **2010**, *382*, 131. (b) Tan, H.; Zhang, P.; Wang, L.; Yang, D.; Zhou, K. *Chem. Commun.* **2011**, *47*, 11903. (c) Xu, X.; Gong, Y.; Zhang, P.; Li, H.; Wang, Y. *J. Am. Chem. Soc.* **2012**, *134*, 16987. (d) Yu, C.; Fan, L.; Yang, J.; Shan, Y.; Qiu, J. *Chem.—Eur. J.* **2013**, *19*, 16192. (e) Teixeira, A. P. C.; Purceno, A. D.; Barros, A. S.; Lemos, B. R. S.; Ardisson, J. D.; Macedo, W. A. A.; Nassor, E. C. O.; Amorim, C. C.; Moura, F. C. C.; Hernandez-Terrones, M. G.; Portela, F. S. M.; Lago, R. M. *Catal. Today* **2012**, *190*, 133. (f) He, Y.; Wu, F.; Sun, X.; Li, R.; Guo, Y.; Li, C.; Zhang, L.; Xing, F.; Wang, W.; Gao, J. *ACS Appl. Mater. Interfaces* **2013**, *5*, 4843.

(10) Leclercq, L.; Mouret, A.; Proust, A.; Schmitt, V.; Bauduin, P.; Aubry, J.-M.; Nardello-Rataj, V. *Chem.—Eur. J.* **2012**, *18*, 14352.

(11) Nakato, T.; Ueda, H.; Hashimoto, S.; Terao, R.; Kameyama, M.; Mouri, E. *ACS Appl. Mater. Interfaces* **2012**, *4*, 4338.

(12) Oliveira, A. A. S.; Teixeira, I. F.; Christofani, T.; Tristao, J. C.; Guimaraes, I. R.; Moura, F. C. C. *Appl. Catal. B: Environ.* **2014**, *144*, 144.

(13) (a) Wu, C.; Bai, S.; Ansorge-Schumacher, M. B.; Wang, D. *Adv. Mater.* **2011**, *23*, 5694. (b) Wang, Z.; van Oers, M. C. M.; Rutjes, F. P. T. J.; van Hest, J. C. M. *Angew. Chem., Int. Ed.* **2012**, *51*, 10746. (c) Liu, J.; Lan, G.; Peng, J.; Li, Y.; Li, C.; Yang, Q. *Chem. Commun.* **2013**, *49*, 9558. (d) Qi, Z.; Wu, C.; Malo de la Molina, P.; Sun, H.; Schulz, A.; Griesinger, C.; Gradzielski, M.; Haag, R.; Ansorge-Schumacher, M. B.; Schalley, C. A. *Chem.—Eur. J.* **2013**, *19*, 10150.

(14) Chan, T. H.; Brook, M. A.; Chaly, T. *Synthesis* **1983**, *3*, 203.

(15) Fan, Z.; Tay, A.; Pera-Titus, M.; Zhou, W.-J.; Benhabbari, S.; Feng, X.; Malcouronne, G.; Bonneviot, L.; De Campo, F.; Wang, L.; Clacens, J.-M. *J. Colloid Interface Sci.* **2014**, DOI: 10.1016/j.jcis.2013.11.047.